Kinetic and Magnetic Resonance Studies of the Role of Metal Ions in the Mechanism of Escherichia coli GDP-mannose Mannosyl Hydrolase, an Unusual Nudix Enzyme †

ARTICLE *in* BIOCHEMISTRY · APRIL 2002

Impact Factor: 3.02 · DOI: 10.1021/bi012118d · Source: PubMed

4 AUTHORS, INCLUDING:

Patricia Legler
United States Naval Research Laboratory
40 PUBLICATIONS **529** CITATIONS

Kinetic and Magnetic Resonance Studies of the Role of Metal Ions in the Mechanism of *Escherichia coli* GDP-mannose Mannosyl Hydrolase, an Unusual Nudix Enzyme†

Patricia M. Legler,‡ H. Caroline Lee,§ Jack Peisach,§ and Albert S. Mildvan*,‡

Department of Biological Chemistry, The Johns Hopkins School of Medicine, 725 North Wolfe Street, Baltimore, Maryland 21205-2185, and Department of Physiology and Biophysics, Albert Einstein College of Medicine, Bronx, New York 10461

Received December 5, 2001; Revised Manuscript Received January 30, 2002

ABSTRACT: *Escherichia coli* GDP-mannose mannosyl hydrolase (GDPMH), a homodimer, catalyzes the hydrolysis of GDP-α-D-sugars to yield the β-D-sugar and GDP by nucleophilic substitution with inversion at the C1′ carbon of the sugar [Legler, P. M., Massiah, M. A., Bessman, M. J., and Mildvan, A. S. (2000) *Biochemistry 39*, 8603−8608]. GDPMH requires a divalent cation for activity such as Mn^{2+} or Mg^{2+}, which yield similar k_{cat} values of 0.15 and 0.13 s^{-1}, respectively, at 22 °C and pH 7.5. Kinetic analysis of the Mn^{2+}-activated enzyme yielded a K_m of free Mn^{2+} of 3.9 ± 1.3 mM when extrapolated to zero substrate concentration ($K_a^{Mn^{2+}}$), which tightened to 0.32 ± 0.18 mM when extrapolated to infinite substrate concentration ($K_m^{Mn^{2+}}$). Similarly, the K_m of the substrate extrapolated to zero Mn^{2+} concentration ($K_S^{GDPmann} = 1.9 \pm 0.5$ mM) and to infinite Mn^{2+} concentration ($K_m^{GDPmann} = 0.16 \pm 0.09$ mM) showed an order of magnitude decrease at saturating Mn^{2+}. Such mutual tightening of metal and substrate binding suggests the formation of an enzyme−metal−substrate bridge complex. Direct Mn^{2+} binding studies, monitoring the concentration of free Mn^{2+} by EPR and of bound Mn^{2+} by its enhanced paramagnetic effect on the longitudinal relaxation rate of water protons (PRR), detected three Mn^{2+} binding sites per enzyme monomer with an average dissociation constant (K_D) of 3.2 ± 1.0 mM, in agreement with the kinetically determined $K_a^{Mn^{2+}}$. The enhancement factor (ϵ_b) of 11.5 ± 1.2 indicates solvent access to the enzyme-bound Mn^{2+} ions. No cross relaxation was detected among the three bound Mn^{2+} ions, suggesting them to be separated by at least 10 Å. Such studies also yielded a weak dissociation constant for the binary Mn^{2+}−GDP-mannose complex ($K_1 = 6.5 \pm 1.0$ mM) which significantly exceeded the kinetically determined K_m values of Mn^{2+}, indicating the true substrate to be GDP-mannose rather than its Mn^{2+} complex. Substrate binding monitored by changes in $^1H-^{15}N$ HSQC spectra yielded a dissociation constant for the binary E−GDP-mannose complex ($K_S^{GDPmann}$) of 4.0 ± 0.5 mM, comparable to the kinetically determined K_S value (1.9 ± 0.5 mM). To clarify the metal stoichiometry at the active site, product inhibition by GDP, a potent competitive inhibitor (K_I = 46 ± 27 μM), was studied. Binding studies revealed a weak, binary E−GDP complex ($K_D^{GDP} = 9.4 \pm 3.2$ mM) which tightened ∼500-fold in the presence of Mn^{2+} to yield a ternary E−Mn^{2+}−GDP complex with a dissociation constant, $K_3^{GDP} = 18 \pm 9$ μM, which overlaps with the K_I^{GDP}. The tight binding of Mn^{2+} to 0.7 ± 0.2 site per enzyme subunit in the ternary E−Mn^{2+}−GDP complex ($K_A' = 15$ μM) and the tight binding of GDP to 0.8 ± 0.1 site per enzyme subunit in the ternary E−Mg^{2+}−GDP complex ($K_3 < 0.5$ mM) indicate a stoichiometry close to 1:1:1 at the active site. The decrease in the enhancement factor of the ternary E−Mn^{2+}−GDP complex ($\epsilon_T = 4.9 \pm 0.4$) indicates decreased solvent access to the active site Mn^{2+}, consistent with an E−Mn^{2+}−GDP bridge complex. Fermi contact splitting (4.3 ± 0.2 MHz) of the phosphorus signal in the ESEEM spectrum established the formation of an inner sphere E−Mn^{2+}−GDP complex. The number of water molecules coordinated to Mn^{2+} in this ternary complex was determined by ESEEM studies in D_2O to be two fewer than on the average Mn^{2+} in the binary E−Mn^{2+} complexes, consistent with bidentate coordination of enzyme-bound Mn^{2+} by GDP. Kinetic, metal binding, and GDP binding studies with Mg^{2+} yielded dissociation constants similar to those found with Mn^{2+}. Hence, GDPMH requires one divalent cation per active site to promote catalysis by facilitating the departure of the GDP leaving group, unlike its homologues the MutT pyrophosphohydrolase, which requires two, or Ap_4A pyrophosphatase, which requires three.

In the presence of Mg^{2+} or Mn^{2+}, the 36.8 kDa homodimeric GDP-mannose mannosyl hydrolase (GDPMH)[1] from *Escherichia coli* catalyzes the hydrolysis of GDP-α-D-mannose or GDP-α-D-glucose to form GDP and the β-sugar.

$$\text{GDP-α-D-mannose} + H_2O \rightarrow \text{GDP} + \text{β-mannose} + H^+ \quad (1)$$

$$\text{GDP-α-D-glucose} + H_2O \rightarrow \text{GDP} + \text{β-glucose} + H^+ \quad (2)$$

Previously, it was shown that the mechanism involved nucleophilic substitution by water at the C1′ carbon of the sugar moiety, with inversion (*1*). Enzymes in the Nudix family of hydrolases catalyze the hydrolysis of nucleoside diphosphate derivatives (NDP-X) and contain the consensus

† This research was supported by National Institutes of Health Grants DK28616 (to A.S.M.) and GM40168 (to J.P.). P.M.L. was supported by a National Science Foundation Graduate Research Fellowship.

* To whom correspondence should be addressed. Phone: 410-955-2038. E-mail: mildvan@welchlink.welch.jhu.edu. Fax: 410-955-5759.

‡ The Johns Hopkins School of Medicine.

§ Albert Einstein College of Medicine.

10.1021/bi012118d CCC: $22.00
Published on Web 03/14/2002

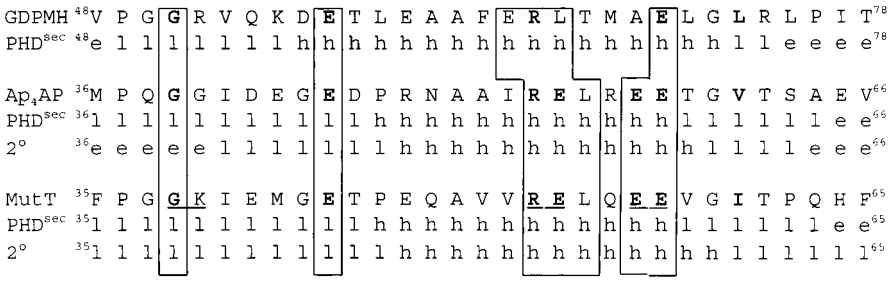

FIGURE 1: Sequence homology of GDPMH, MutT pyrophosphohydrolase, and Ap_4A pyrophosphatase. Beneath the sequences are the PHD secondary structure predictions (*36*), where h = helical, e = extended (sheet), and l = loop. The secondary structures of the MutT pyrophosphohydrolase (*5*, *37*) and of the *Lupinus angustifolius* L. Ap_4AP (*6*) determined by NMR are denoted by 2°. Bold residues are highly conserved in the Nudix family of enzymes. Underlined residues are in the active site of MutT.

sequence **G**$(X)_5$E$(X)_7$**RE**UXE**E**XGU, where U is a hydrophobic residue and the bold residues are highly conserved (*2*). All Nudix enzymes have been shown to catalyze nucleophilic substitutions at phosphorus, on the bases of their reaction products and, in some cases, by direct ^{18}O incorporation studies (*3*, *4*), with the exception of GDPMH, which catalyzes nucleophilic substitution at carbon (*1*).

The difference in mechanism may be attributable to sequence differences in the Nudix motif of GDPMH. GDPMH shares homology with the Nudix family of enzymes but contains a reversal in the consensus sequence, ER instead of RE, and lacks a conserved glutamate residue corresponding to a metal-liganding residue, Glu 56, of MutT (Figure 1). In the MutT pyrophosphohydrolase, the prototypical Nudix enzyme, the consensus sequence forms a novel loop−helix−loop motif, which serves as the binding site for an essential divalent cation and the triphosphate moiety of the NTP substrate (*5*). A similar loop−helix−loop motif was found with the Nudix enzyme Ap_4A pyrophosphatase (*6*) and is predicted for GDPMH (Figure 1).

From kinetic studies, compared with direct measurements of metal and substrate binding affinities, it was shown that the MutT enzyme requires two divalent cations for activity, one bound to the NTP substrate and one bound to the enzyme (*7*). Another Nudix enzyme, Ap_4A pyrophosphatase, was shown to require three divalent cations for activity, one bound to the substrate and the other two bound near one another on the enzyme (*8*). This paper extends such measurements to the unusual Nudix enzyme, GDPMH, to determine the stoichiometry and precise roles of divalent cations. In addition, electron spin−echo envelope modulation (ESEEM) spectroscopy was used to examine the ligands of Mn^{2+} in the active site (*9*, *10*). Fermi contact interaction of the unpaired electrons of Mn^{2+} with the phosphates of the GDP product in the ternary enzyme−Mn^{2+}−GDP complex was observed, establishing direct phosphate coordination to the enzyme-bound divalent cation. ESEEM experiments were also used to compare the number of water ligands on Mn^{2+} in the binary enzyme−Mn^{2+} complexes and the ternary enzyme−Mn^{2+}−GDP complex.

EXPERIMENTAL PROCEDURES

Materials. The nucleotides GDP and GDP-α-D-mannose were purchased from Sigma. Nucleotide and buffer solutions were passed over Chelex 100 resin to remove trace metal contaminants. Analytical grade Chelex 100 was purchased from Bio-Rad Laboratories (Richmond, CA). SigmaUltra ammonium sulfate and MES buffer were also purchased from Sigma (St. Louis, MO). HEPES and MOPS buffers were purchased from Fisher Scientific (Fair Lawn, NJ). Ultrapure (99.995%) $MnCl_2$ was purchased from Johnson Matthey Chemicals Ltd. (London, England). Ultrapure (99.995%) $MgCl_2$ hexahydrate, ethylene glycol, and 2-methylbutane were purchased from Aldrich Chemical Co. (Milwaukee, WI). Ultrapure cobalt(II) chloride was purchased from Alfa Aesar (Ward Hill, MA). Ultrafiltration concentrators (polyether sulfone membrane, 10000 MWCO) were purchased from Vivascience (Gloucestershire, U.K.). The BCA protein determination kit was from Pierce (Rockford, IL). Ecolite-(+) scintillation cocktail was from ICN Biomedicals, Inc. (Costa Mesa, CA). *E. coli* strain BL-21(DE3) Epicurian Coli was purchased from Stratagene (La Jolla, CA). AEBSF and calf intestinal alkaline phosphatase were purchased from Roche Diagnostics Co. (Indianapolis, IN). ^{15}N-Labeled ammonium chloride was purchased from Isotec (Miamisburg, OH). The d_2-ethylene glycol was purchased from Cambridge Isotope Laboratories, Inc. (Andover, MA). ^3H-Labeled GDP-mannose was purchased from NEN Life Science Products (Boston, MA). The nonexchangeable tritium was present on the C2′ of the mannose moiety. The tritiated GDP-mannose was supplied in 70% ethanol and was lyophilized before use.

General Methods. For protein expression, *E. coli* strain BL-21(DE3) cells containing the petGDPMH plasmid were grown in MOPS media (*11*) with either unlabeled or ^{15}N-labeled ammonium chloride in the presence of 100 μg/mL ampicillin at 37 °C. The construction of the petGDPMH plasmid and purification of the GDPMH enzyme were described previously (*12*). The enzyme used in these experiments was additionally desalted on a G-25 Sephadex column (22 cm × 1 cm) to remove EDTA which was present in the buffers used in the purification protocol. Before and after desalting, the enzyme was concentrated using Vivaspin ultrafiltration concentrators. For $^1H-^{15}N$ HSQC studies, the buffer of the ^{15}N-labeled enzyme was exchanged into 5.4 mM d_{11}-Tris, pH 7.5, 18 mM NaCl, 0.3 mM NaN_3, 10 mM DTT, 0.1 mg/mL AEBSF, and 10% D_2O by three cycles of

[1] Abbreviations: AEBSF, 4-(2-aminoethyl)benzenesulfonyl fluoride; Ap_4AP, diadenosine pyrophosphatase; BCA, bicinchoninic acid: DTPA, diethylenetriaminepentaacetic acid; EDTA, (ethylenedinitrilo)tetraacetic acid; EPR, electron paramagnetic resonance; ESEEM, electron spin−echo envelope modulation; FID, free induction decay; GDP, guanosine diphosphate; GDPMH, GDP-mannose mannosyl hydrolase; HSQC, heteronuclear single-quantum coherence; LB/Amp, Luria−Bertani medium containing ampicillin; MES, 2-(*N*-morpholino)ethanesulfonic acid; MWCO, molecular weight cutoff; NMR, nuclear magnetic resonance; PRR, proton relaxation rate; RF, radio frequency; TPPI, time-proportional phase incrementation.

concentration and dilution using the 6 mL ultrafiltration concentrators. The concentration of GDPMH was determined spectrophotometrically using $\epsilon_{280}^{native} = 72.8\ mM^{-1}\ cm^{-1}$ at pH 6.5 in 20 mM phosphate buffer (*13*) and by the BCA assay using BSA as the standard. The two methods differed by 3% for the GDPMH protein. The concentrations of GDP and GDP-mannose were determined using $\epsilon_{252.5} = 13.6\ mM^{-1}\ cm^{-1}$ at pH 6.0 in 50 mM MES buffer.

Kinetic Studies. Steady-state kinetic experiments with either Mg^{2+}- or Mn^{2+}-activated GDPMH were performed by measuring the amount of phosphate produced when the product, GDP, was treated with calf intestinal alkaline phosphatase. Alkaline phosphatase does not cleave the GDP-α-D-mannose substrate. The reactions proceeded at 22 °C, pH 7.5, for 20 min and contained approximately 0.5 μg of enzyme (~0.001 unit). Under these conditions activity was linear with time. The 50 μL reactions were terminated by heating at 95 °C for 3 min. The reactions were then treated with 1 unit of alkaline phosphatase for 11 min at 37 °C, followed by addition of 250 μL of 5 mM EDTA. A 700 μL volume of Ames Mix (1 part 10% ascorbic acid to 6 parts 0.42% ammonium molybdate in 1 N H_2SO_4) was then added to the reaction mixtures, and the reactions were heated for 30 min at 37 °C. The concentration of phosphomolybdate was determined at 780 nm using potassium phosphate as a standard.

For the measurement of the K_I of GDP, GDP-α-D-mannose containing tritium on the 2′ carbon of the mannose moiety was added to unlabeled substrate to yield a solution of GDP-mannose containing highly labeled ^{3}H-GDP-mannose (2.7 μCi/μmol). Reactions (in 50 μL) contained 80 mM HEPES, pH 7.5, 20 mM $MnCl_2$, 0.8 μg (~1.4 milliunits) of enzyme, and 0.30 or 0.60 mM GDP-mannose. The concentrations of GDP were 0.0, 0.06, 0.08, 0.10, and 0.12 mM with the former substrate concentration and 0.0, 0.08, 0.10, 0.12, 0.14, and 0.16 mM GDP with the latter substrate concentration. For the measurement of the K_I^{GDP} in the presence of Mg^{2+}, 0.47 or 0.62 mM GDP-mannose was used, and GDP concentrations of 0.0, 0.05, 0.06, and 0.08 mM were used in the former case and 0.0, 0.06, 0.08, and 0.10 mM in the latter case. Assays were carried out for 2 min at 22 °C, quenched with 7% perchloric acid (20 μL), and treated with an aqueous 40% (w/v) acid-washed Norit charcoal suspension (100 μL) to adsorb the GDP product and the unreacted ^{3}H-GDP-mannose. The samples were chilled on ice for 5 min, and charcoal was removed by centrifugation and recentrifugation of the supernatant. The supernatant (100 μL) which contained the cleaved [^{3}H]mannose product was then added to 3.5 mL of scintillation fluid and counted. The amount of GDP produced in the GDPMH-catalyzed reaction did not exceed 21% of the concentration of the added GDP used as the inhibitor.

Mn^{2+} Binding Studies. The concentration of free Mn^{2+} in a mixture of free and bound Mn^{2+} was measured by EPR at 22 °C on a Varian E-4 EPR spectrometer operating at X-band (9.1 GHz), as previously described (*14*, *15*). The symmetry of the ligand field in $Mn(H_2O)_6^{2+}$ results in a degeneracy of the five electronic transitions in this $S = {}^5/_2$ system, leading to a six-line spectrum due to hyperfine interaction with the nuclear spin of Mn ($I = {}^5/_2$). The replacement of one or more water ligands on Mn^{2+} by a different ligand perturbs the symmetry of the ligand field, abolishing the degeneracy of the five electronic transitions, broadening the overall EPR spectrum such that, at room temperature, it largely disappears into the baseline (*16*).

Bound Mn^{2+} was monitored by the longitudinal proton relaxation rate (PRR) of water, $1/T_1$. A $180°-\tau-90°$ pulse sequence was used to measure $1/T_1$. PRR data were collected using a Seimco pulsed NMR spectrometer operating at 24.3 MHz as previously described (*14*).

Binding to the enzyme enhanced the paramagnetic effects of Mn^{2+} on the longitudinal relaxation rate of water protons in the binary and ternary complexes in PRR experiments. The observed enhancement, ϵ^*, is defined as

$$\epsilon^* = \frac{(1/T_1)^* - (1/T_1)_0^*}{(1/T_1) - (1/T_1)_0} \tag{3}$$

where $(1/T_1)$ and $(1/T_1)_0$ are the longitudinal relaxation rates of water protons in the presence and absence of Mn^{2+}, respectively, and the asterisks indicate the presence of the macromolecule, GDPMH. Observed enhancements greater than 1 are due to an increase in the correlation time τ_c for the dipolar interaction between Mn^{2+} and its coordinated water ligands, resulting from restricted rotational motion of the coordination sphere of the bound metal ion (*17*−*19*).

The dissociation constant of the binary Mn^{2+}−GDP-mannose complex was determined by both PRR and EPR. The ratio of $[Mn^{2+}]_{free}$ to $[Mn^{2+}]_{total}$ was determined by EPR, and the amount bound was calculated using the known $[Mn^{2+}]_{total}$ concentration. It has previously been shown that the observed enhancement, ϵ^*, is the weighted sum of all of the Mn^{2+}-containing species present.

$$\epsilon^* = \sum_i \frac{[Mn]_i}{[Mn]_{total}} \epsilon_i \tag{4}$$

Using the observed enhancement, ϵ^*, determined by PRR, the enhancement due to bound Mn^{2+}, ϵ_b, was determined with the equation:

$$\epsilon^* = \frac{[Mn^{2+}]_F}{[Mn^{2+}]_T}\epsilon_f + \frac{[Mn^{2+}]_B}{[Mn^{2+}]_T}\epsilon_b \tag{5}$$

The enhancement of free Mn^{2+}, ϵ_f, is defined as unity. Rearrangement of eq 5 and substitution of $[Mn^{2+}]_B = [Mn^{2+}]_T - [Mn^{2+}]_F$ yields the equation:

$$\frac{[Mn^{2+}]_F}{[Mn^{2+}]_T} = \frac{\epsilon_b - \epsilon^*}{\epsilon_b - 1} \tag{6}$$

Seven measured ϵ_b values were averaged and used to back-calculate $[Mn^{2+}]_F$. The dissociation constants determined from the EPR measurements and the observed enhancements agreed and were averaged.

The dissociation constant and binding stoichiometry of the binary Mn^{2+}−GDPMH complex were determined by Scatchard analysis. Observed enhancements were used to calculate an average ϵ_b, and the $[Mn^{2+}]_F$ was back-calculated from both EPR and PRR data using eq 6. Dissociation constants and stoichiometries of the enzyme−Mn^{2+}−GDP complex were also determined by Scatchard analysis. Observed enhancements were used to calculate an average

ϵ_T value, and the $[Mn^{2+}]_F$ was back-calculated using an equation analogous to eq 6, where the concentration of the binary E−Mn^{2+} complex was negligible.

Mg^{2+} Binding Studies. Because Mg^{2+} is diamagnetic, its binding cannot be directly observed by PRR. Hence the dissociation constant of the binary enzyme−Mg^{2+} complex was determined by PRR titration by competition with Mn^{2+}. A recipient solution containing 0.46 mM GDPMH subunits, 0.485 mM $MnCl_2$, and 80 mM NaHEPES, pH 7.5, was titrated with an otherwise identical solution which also contained 5 mM $MgCl_2$. In a second titration the recipient solution (40 μL) was identical to the one above, but was titrated with 100 mM $MgCl_2$. The 25% dilution of the enzyme was taken into account in computing the dissociation constant of Mg^{2+}.

$^1H-^{15}N$ HSQC Spectral Titrations of GDPMH. The binding of Mg^{2+} and nucleotides to GDPMH alter the chemical shifts of the backbone ^{15}N and $^1H(N)$ resonances in $^1H-^{15}N$ HSQC spectra, permitting independent measurements of the dissociation constants of Mg^{2+} and nucleotides in the binary and ternary complexes even though the cross-peaks are unassigned. All NMR spectra were collected at 21.5 °C on a Varian Unity Plus 600 MHz NMR spectrometer equipped with a pulse field gradient unit and four independent RF channels. The HSQC spectra were collected with a Varian 5 mm triple resonance probe with an actively shielded *z*-gradient. The States−TPPI method was employed in the indirect dimension for the two-dimensional $^1H-^{15}N$ HSQC spectra (*20*). Both Mg^{2+} and GDP binding to GDPMH showed fast exchange, averaging chemical shifts between free and bound enzyme, except where noted. Absolute values of chemical shift changes ($\Delta\delta_{obs}$) were plotted against the total concentration of the titrant. The dissociation constant (K_D) was determined using the equation:

$$\Delta\delta_{obs} = \frac{\Delta\delta_{max}[(K_D + L_t + E_t) - \sqrt{(K_D + L_t + E_t)^2 + 4L_tE_t}]}{2E_t} \quad (7)$$

in which $\Delta\delta_{max}$ is the maximal chemical shift change, L_t is the total ligand concentration, and E_t is the total enzyme subunit concentration. Equation 7 takes into account the dilution of the enzyme by substrate additions over the course of the titration.

GDPMH (1.31 mM) was titrated with 0.99−21.85 mM $MgCl_2$ in six steps to measure the $K_D^{Mg^{2+}}$; the pH was maintained at 7.54 ± 0.05. The chemical shifts of eight cross-peaks, all of which showed maximal chemical shift changes ($\Delta\delta_{max}$) greater than 0.12 ppm, were followed and used to calculate the dissociation constant. After titration with Mg^{2+}, the sample (0.98 mM GDPMH, 21.85 mM Mg^{2+}) was then titrated with GDP in six steps over a range of concentrations (0.103−2.09 mM). To avoid dilution of the Mg^{2+}, a 25 mM titrant solution of Mg^{2+}−GDP was made using equimolar concentrations of GDP and $MgCl_2$. Slow exchange and tight binding of GDP were observed for this titration, precluding measurement of the dissociation constant of GDP from the ternary complex, K_3^{GDP}. Instead, increases in peak volume of the ternary enzyme−Mg^{2+}−GDP complex species and decreases in peak volume of the binary E−Mg^{2+} species were followed over the course of the titration to yield the binding stoichiometry of GDP to the enzyme−Mg^{2+} complex. Seven peak pairs were used to determine the binding stoichiometry.

In a third titration experiment 1.18 mM GDPMH was titrated with 0.96−21.24 mM GDP in six steps to measure K_S, the dissociation constant of the binary enzyme−GDP complex, with the pH maintained at 7.55 ± 0.02. The changing chemical shifts of 11 peaks were followed, which showed $\Delta\delta_{max} \geq 0.16$ ppm. In a fourth titration 1.02 mM GDPMH containing 1.1 mM GDP was titrated with 0.050−4.0 mM Mg^{2+} in an attempt to measure the K_A'. Slow exchange and tight binding of the metal were observed, precluding measurement of the dissociation constant of Mg^{2+} from the enzyme−GDP complex. Four new peaks were followed during the course of the titration and were used to calculate the binding stoichiometry of Mg^{2+} to the enzyme−GDP complex. In a fifth titration, GDPMH (1.12 mM) was titrated with 0.27−14.52 mM GDP-mannose in six steps, with the pH maintained at 7.54 ± 0.07. Seven peaks with $\Delta\delta_{max}(^{15}N) \geq 0.25$ ppm were used to calculate the dissociation constant of the binary enzyme−substrate complex, $K_S^{GDP-mannose}$.

Low-Temperature EPR and Electron Spin−Echo Envelope Modulation Spectroscopy. Continuous wave EPR spectra were collected at X-band, at liquid nitrogen temperature (77 K), on a Varian E-112 spectrometer equipped with a Systron-Donner frequency counter and a PC-based data acquisition program. ESEEM data were collected at X-band, at liquid helium temperature (4 K), on a home-built pulsed EPR spectrometer (*21, 22*) using a folded strip-line cavity (*23*). Two-pulse data (*24*) were collected at time 2τ (where τ is the interval between the first and the second microwave pulses), with τ incrementing from 140 ns in steps of 5 ns. Three pulse data (*25*) were collected at time $2\tau + T$ (where T is the interval between the second and third microwave pulses), with T incrementing from 60 ns in steps of 10 ns. Each data set contained 1024 points. ESEEM spectra presented in Figures 8 and 9 are cosine Fourier transforms of the time-domain data. Sample volumes were 150 or 200 μL. The samples were frozen in liquid nitrogen-cooled isopentane and then stored in liquid nitrogen.

Ethylene glycol, a magnetic diluent, gave a homogeneous glassy sample upon freezing. Without ethylene glycol, FIDs trailed off more rapidly, limiting the amount of low-frequency data that could be collected. The effects of ethylene glycol on the k_{cat} and K_m of the GDPMH enzyme were measured at 0 and 22 °C.

Samples of the binary enzyme−Mn^{2+} complex contained 1.0 mM Mn^{2+}, 2.9 mM GDPMH subunits, and 80.0 mM NaHEPES, pH 7.5, in either the presence or absence of 1:1 (v/v) ethylene glycol. Samples of the ternary enzyme−Mn^{2+}−GDP complex were made in the presence and absence of 1:1 (v/v) ethylene glycol to determine the effect of ethylene glycol on the Fermi contact splitting. These samples contained 1.0 mM Mn^{2+}, 2.9 mM GDPMH enzyme subunits, 2.24 mM GDP, and 80.0 mM NaHEPES, pH 7.5. From the dissociation constant of Mn^{2+} from its tight binding site ($K_A' = 15$ μM), at least 98% of the Mn^{2+} was calculated to be bound in the ternary enzyme−Mn^{2+}−GDP complex. The corresponding samples in D_2O contained 1.0 mM Mn^{2+}, 2.6 mM GDPMH subunits, with and without 2.24 mM GDP, and 80 mM NaHEPES, pH 7.5 in 1:1 (v/v) 99.9% D_2O and d_2-ethylene glycol. The enzyme was exchanged into 80 mM

NaHEPES (in 99.9% D_2O) using Vivaspin ultrafiltration units. The pH values of the GDP and HEPES solutions were adjusted to 7.5 in H_2O and then lyophilized. The lyophilized GDP and HEPES were redissolved in 99% D_2O, lyophilized three times, and finally redissolved in 99.9% D_2O.

The model compounds, Mn^{2+}-EDTA and Mn^{2+}-DTPA, were prepared with a slight excess of chelator and contained 1.2 mM EDTA or DTPA, 1.0 mM $MnCl_2$, 80 mM Na-HEPES, pH 7.5, in H_2O or in 99.9% D_2O and 1:1 (v/v) ethylene glycol or d_2-ethylene glycol. The solutions of the small molecules were initially prepared in H_2O, and the pH was adjusted prior to lyophilization. The solutions were lyophilized and redissolved in 99% D_2O three times and finally redissolved in 1:1 (v/v) 99.9% D_2O and d_2-ethylene glycol.

The two-pulse experiment was used to observe the ^{31}P Fermi contact splitting in the binary Mn^{2+}−GDP and ternary enzyme−Mn^{2+}−GDP complexes in H_2O, as previously described (*9*). Quantitation of changes in the number of water ligands coordinated to the enzyme-bound Mn^{2+} by ESEEM utilized a previously established ^2H ESEEM method (*9*). The three-pulse experiment was used to obtain more accurate measurements of the deuterium peak intensities. ^2H ESEEM data were isolated by ratioing the normalized time-domain data of a sample in D_2O solvent with the normalized time-domain data of an otherwise identical sample in H_2O solvent, to remove underlying ^{14}N and ^{31}P signals. The predominant signal in the Fourier transform of the ^2H ESEEM data was the peak at the deuterium Larmor frequency, due to both directly coordinated and nearby water in the second and higher coordination spheres.

The difference between the average number of Mn^{2+}-bound D_2O ligands in the binary enzyme−Mn^{2+} and ternary enzyme−Mn^{2+}−GDP complexes was obtained by ratioing the ^2H ESEEM data of these two complexes, assuming the contribution of ambient D_2O to the ^2H ESEEM of both complexes to be the same, and comparing the intensity of the ^2H peak to that of standard Mn^{2+} complexes with known numbers of D_2O ligands (see Results). From their X-ray structures, Mn^{2+}-EDTA shows one water ligand on the metal, and Mn^{2+}-DTPA shows no water ligands (*26*). The ^2H ESEEM of Mn^{2+}-EDTA was ratioed with that of Mn^{2+}-DTPA to obtain the ^2H ESEEM of the single Mn^{2+}-bound D_2O in Mn^{2+}-EDTA, assuming that the modulations due to ambient D_2O in both complexes are the same (*9*). These assumptions were previously found to be valid in comparing binary and ternary Mn^{2+} complexes of staphylococcal nuclease (*9*).

RESULTS

Kinetic Studies of Manganese-Activated GDPMH. The effects of varying metal and substrate concentrations on the initial rates of hydrolysis of GDP-mannose were measured. All of the data were simultaneously well fit ($\chi^2 = 0.00075$) to a general rate equation for a metal-activated enzyme with a random order mechanism (eq 8) to evaluate the five kinetic

$$v = (V_{max}[M^{2+}][\text{GDP-mannose}]_{free})/ (\beta K_a^{M^{2+}} K_S^{GDPmann} + \beta K_a^{M^{2+}}[\text{GDP-mannose}]_{free} + \beta K_S^{GDPmann}[M^{2+}] + [M^{2+}][\text{GDP-mannose}]_{free}) \quad (8)$$

Scheme 1

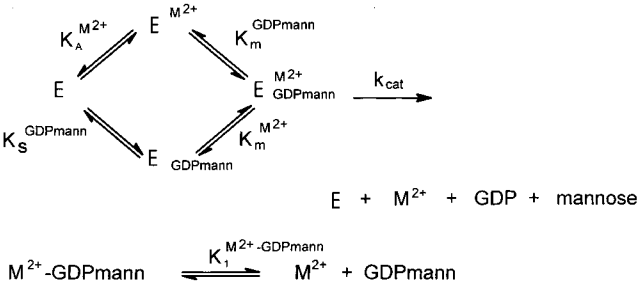

parameters defined in Scheme 1. In eq 8, β is a proportionality constant used in describing the following relationships for the thermodynamic box in Scheme 1:

$$K_m^{M^{2+}} = \beta K_a^{M^{2+}} \quad (9)$$

$$K_m^{GDPmann} = \beta K_S^{GDPmann} \quad (10)$$

A double reciprocal plot of the kinetic data with varying Mn^{2+} and GDP-mannose is shown in Figure 2 , and the five parameters determined by simultaneously fitting the data are given in Table 1. It is noteworthy that substrate binding lowered the K_m of free Mn^{2+} by an order of magnitude, and Mn^{2+} binding lowered the K_m of the free substrate by an order of magnitude, suggesting the formation of an enzyme−Mn^{2+}−substrate bridge complex. These experiments were repeated many times, and the errors in the parameters reflect the consistency of the data.

Kinetic Studies of Magnesium-Activated GDPMH. Kinetic data for the Mg^{2+}-activated enzyme were also collected and analyzed as above. As with Mn^{2+}, the experiments with Mg^{2+} were repeated many times, and the errors in the parameters reflect the consistency of the data. Interestingly, the kinetic parameters with Mg^{2+} (Table 1) were not significantly different from those of the Mn^{2+}-activated enyzme, despite the fact that Mn^{2+} generally binds ligands more tightly than Mg^{2+} does (*27*). This unusual behavior is unprecedented in Nudix enzymes (*7*, *8*).

Measurement of K_I^{GDP} with Mn^{2+}- or Mg^{2+}-Activated GDPMH. Because a nonhydrolyzable substrate was unavailable, product complexes were studied. No product inhibition by glucose or mannose at concentrations up to 20 mM was detected, indicating that the K_I values of both sugars exceeded 20 mM. However, significant inhibition by GDP was found. The K_I of the inhibitory product GDP was measured using a highly sensitive assay with tritium-labeled substrate, as described in Experimental Procedures. The data were plotted and analyzed according to Dixon (Figure 3) (*28*). GDP was shown to be a linear competitive inhibitor with a measured $K_I^{GDP} = 46 \pm 27$ μM with Mn^{2+} activation and $K_I^{GDP} = 56 \pm 23$ μM with Mg^{2+} activation (Table 1).

Binary Enzyme−GDP-mannose and Enzyme−GDP Complexes. The dissociation constant of the GDP-mannose substrate from the enzyme in the absence of metal ions, $K_S^{GDPmann}$, was measured in a $^1H-^{15}N$ HSQC NMR titration experiment, which yielded a value of 4.0 ± 0.5 mM (Figure 4A, Table 2). This value is comparable to the kinetically determined values of $K_S^{GDPmann} = 1.9 \pm 0.5$ mM and $1.4 \pm$

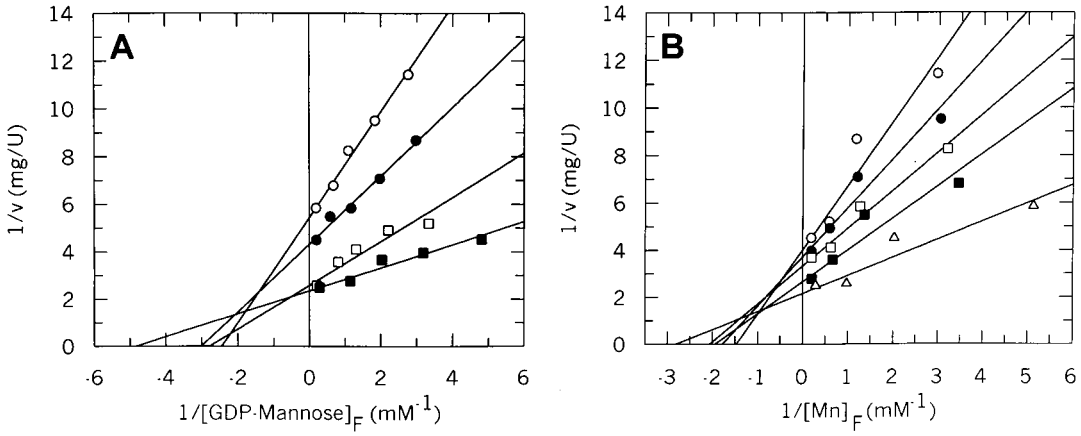

FIGURE 2: Kinetics of Mn^{2+} activation of GDPMH at 22 °C, pH 7.5. (A) Double reciprocal plot of initial velocity versus free substrate concentration at the following (mM) concentrations of $MnCl_2$: (○) 0.357, (●) 0.893, (□) 1.786, (■) 5.358. Other components present were 80 mM NaHEPES, pH 7.5, and 1 unit of calf intestinal alkaline phosphatase. (B) Double reciprocal plot of initial velocity versus free Mn^{2+} concentration at the following (mM) concentrations of GDP-mannose: (○) 0.38, (●) 0.57, (□) 0.96, (■) 1.53, and (△) 5.34. Velocity, expressed as units/mg may be converted to turnover number (s^{-1}) by the factor 0.307. The lines were obtained by weighted least-squares fitting of the data.

Table 1: Kinetically Determined Constants for GDPMH at 22 °C and pH 7.5[a]

enzyme	metal	K_a^{M2+} (mM)	K_m^{M2+} (mM)	$K_S^{GDPmann}$ (mM)	$K_m^{GDPmann}$ (mM)	K_I^{GDP} (mM)	k_{cat} (s^{-1})
wt	Mn^{2+}	3.9 ± 1.1	0.32 ± 0.18	1.9 ± 0.5	0.16 ± 0.09	0.046 ± 0.027[b]	0.15 ± 0.01
wt	Mg^{2+}	3.9 ± 1.3	0.69 ± 0.42	1.4 ± 0.4	0.24 ± 0.14	0.056 ± 0.023[b]	0.13 ± 0.01

[a] Kinetic constants are defined in Scheme 1. [b] Determined by radioactive assay as described in Experimental Procedures.

Table 2: Summary of Dissociation Constants (mM) for the Enzyme−M^{2+}−GDP-mannose and Enzyme−M^{2+}−GDP Complexes Obtained by NMR PRR and EPR

parameter	M = Mn^{2+}	average	M = Mg^{2+}	average	no metal
		A = GDP-mannose			
K_1 = [A][M]/[AM]	6.2 ± 0.4[a] 6.7 ± 0.9[b]	6.5 ± 1.0	9.1 ± 2.0		
K_S = [E][A]/[EA]					4.0 ± 0.5
		A = GDP			
K_1 = [A][M]/[AM]	0.12 ± 0.04		0.4[c]		
K_2 = [E][AM]/[EMA]	0.5 ± 0.3				
K_3 = [EM][A]/[EMA]	0.018 ± 0.009[b]		<0.5[d]		
K_D = [E][M]/[EM]	3.2 ± 1.0 (n = 3.1 ± 0.9)		4.6 ± 0.5[e] 4.8 ± 1.1[f] 8.6 ± 1.5[d]	6.0 ± 1.8	
K_A' = [EA][M]/[EMA]	0.015 ± 0.003 (n = 0.7 ± 0.2) 2.6 ± 0.4 (n = 10 ± 5)		<0.3[d]		
K_S = [E][A]/[EA]					9.4 ± 3.2[d]

[a] Determined by EPR. [b] Determined by EPR and PRR. [c] From ref *27*. [d] From $^1H-^{15}N$ HSQC titration. [e] From PRR titration in competition with Mn^{2+}. [f] From PRR titration in competition with Mn^{2+}, allowing dilution of the enzyme.

0.4 mM with Mn^{2+} and Mg^{2+}, respectively, each extrapolated to zero metal concentration (Table 1). Dissociation constants obtained by kinetics are compared with those obtained by binding studies in Table 3.

The dissociation constant of the product, GDP, from the enzyme in the absence of metal ions, K_S^{GDP}, was also measured by a $^1H-^{15}N$ HSQC NMR titration experiment and yielded a value of 9.4 ± 3.2 mM, approximately 2-fold weaker than the substrate (Figure 4B). This weak binding in the absence of the divalent cation may be due to the lack of charge neutralization of several conserved glutamate residues including Glu 70, which corresponds to the metal ligand, Glu 57, in MutT (*29*).

Binary Enzyme−Mn^{2+} Complexes. The dissociation constant of the enzyme−Mn^{2+} complex was measured by both EPR, which measures free Mn^{2+}, and PRR, which monitors a property of bound Mn^{2+}. The Scatchard plot (Figure 5A) revealed 3.1 ± 0.9 Mn^{2+} binding sites per subunit with an average dissociation constant K_D = 3.2 ± 1.0 mM (Table

Table 3: Comparison of Dissociation Constants (mM) Determined by Kinetics and by Binding Studies[a]

kinetics		binding	
K_a^{Mn2+}	3.9 ± 1.1	K_D^{Mn2+}(E−M)	3.2 ± 1.0
K_a^{Mg2+}	3.9 ± 1.3	K_D^{Mg2+}(E−M)	6.0 ± 1.8
K_I^{GDP}(Mn^{2+})	0.046 ± 0.027	K_3(GDP)(Mn^{2+})	0.018 ± 0.009
K_I^{GDP}(Mg^{2+})	0.056 ± 0.023	K_3(GDP)(Mg^{2+})	<0.5[b]
$K_S^{GDPmann}$(Mn^{2+})	1.9 ± 0.5	$K_S^{GDPmann}$	4.0 ± 0.5
$K_S^{GDPmann}$(Mg^{2+})	1.4 ± 0.4	$K_S^{GDPmann}$	4.0 ± 0.5

[a] The kinetic parameters are defined in Scheme 1, and the dissociation constants are defined in Table 2. [b] A stoichiometric titration was obtained at 0.98 mM GDPMH subunits, indicating the K_3 value to be well below 0.5 mM.

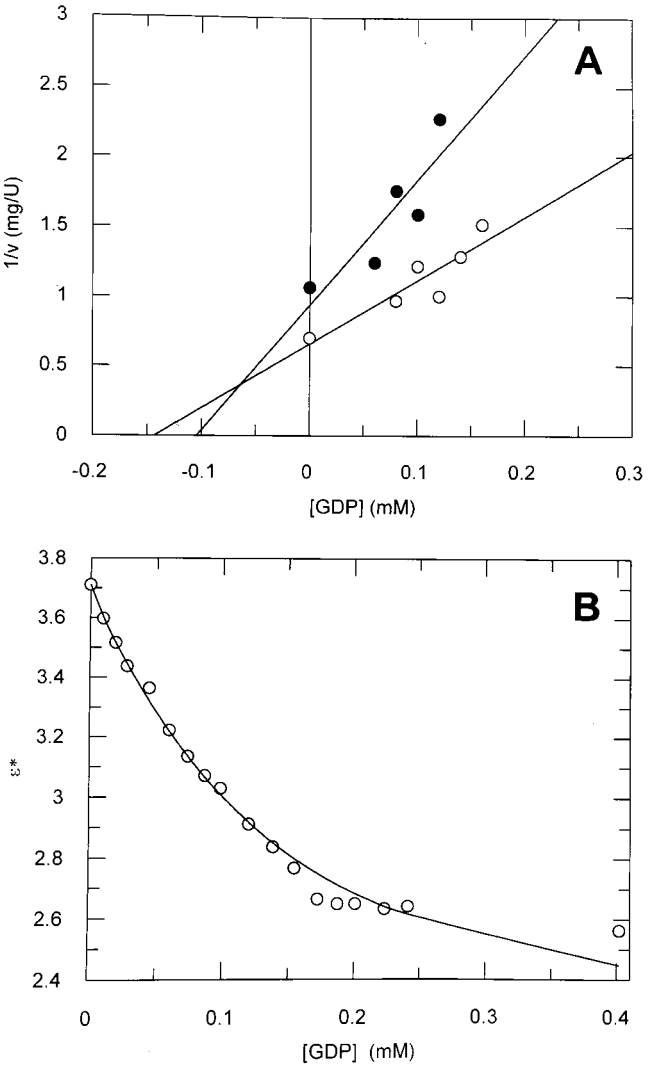

FIGURE 3: Binding of GDP to the GDPMH−Mg^{2+} and GDPMH−Mn^{2+} complexes. (A) Dixon plot of kinetic data for the determination of the K_I of GDP with Mg^{2+} activation at 22 °C, pH 7.5. The substrate concentrations were (●) 0.30 mM GDP-mannose and (○) 0.60 mM GDP-mannose. The GDP concentrations were 0.0, 0.06, 0.08, 0.10, and 0.12 mM with 0.30 mM substrate and 0.0, 0.08, 0.10, 0.12, 0.14, and 0.16 mM with 0.60 mM substrate. (B) PRR titration of GDPMH (496 μM subunits) and $MnCl_2$ (101.3 μM) with GDP maintaining constant concentrations of all components other than GDP. Also present was 80 mM NaHEPES, pH 7.5. The computed curve fit to the data is for a K_3 value of 18 μM and an ϵ_T value of 4.5. Other determinations yielded an overall average ϵ_T value of 4.9 ± 0.4.

2). This K_D value agrees with the kinetically determined activator constant of Mn^{2+} ($K_A^{Mn^{2+}} = 3.9 \pm 1.1$ mM) (Table 1), indicating that at least one of the three Mn^{2+} binding sites functions in catalysis. The average enhancement factor (ϵ_b) of 11.5 ± 1.2 was calculated for these three sites using eq 5 (Table 4). This value of ϵ_b clearly exceeds 1, indicating that the bound Mn^{2+} ions retain water ligands and that the correlation time for Mn^{2+}−water proton dipolar interaction has increased significantly (*18*). A constant value of ϵ_b as a function of occupancy of the Mn^{2+} binding sites was observed, arguing against dipolar interactions between the bound Mn^{2+} ions, indicating that they bind at least 10 Å from each other (*8*).

Binary Mn^{2+}−Nucleotide Complexes. The dissociation constant of the binary Mn^{2+}−GDP-mannose complex (K_1) was measured directly by titration of GDP-mannose with Mn^{2+} monitored by both PRR and EPR. The high dissociation constant of the Mn^{2+}−GDP-mannose complex, $K_1 = 6.5 \pm 1.0$ mM (Table 2), was 20 times greater than the K_m of Mn^{2+} (0.32 ± 0.18 mM) (Table 1), suggesting that GDP-mannose alone binds to the enzyme rather than as a metal−

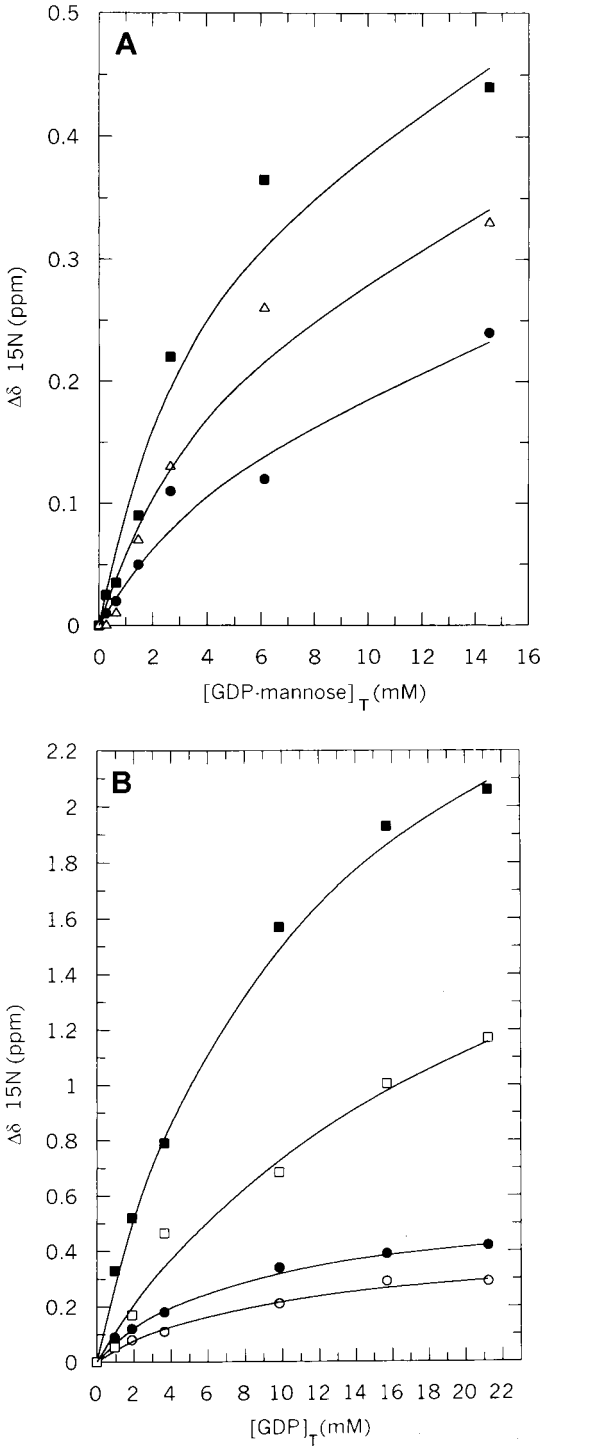

FIGURE 4: $^1H-^{15}N$ HSQC titration of GDPMH with nucleotides monitored by changes in ^{15}N chemical shifts of the enzyme in the absence of metal ions. (A) GDP-mannose titration. The initial chemical shifts in ppm for ^1H and ^{15}N were 8.15, 120.38 (●), 6.07, 111.36 (△), and 8.68, 119.19 (■). (B) GDP titration. The initial chemical shifts in ppm for ^1H and ^{15}N were 8.21, 104.18 (○), 8.00, 126.44 (●), 8.03, 106.85 (□), and 8.00, 126.44 (■). The curves are fitted to the data using eq 7.

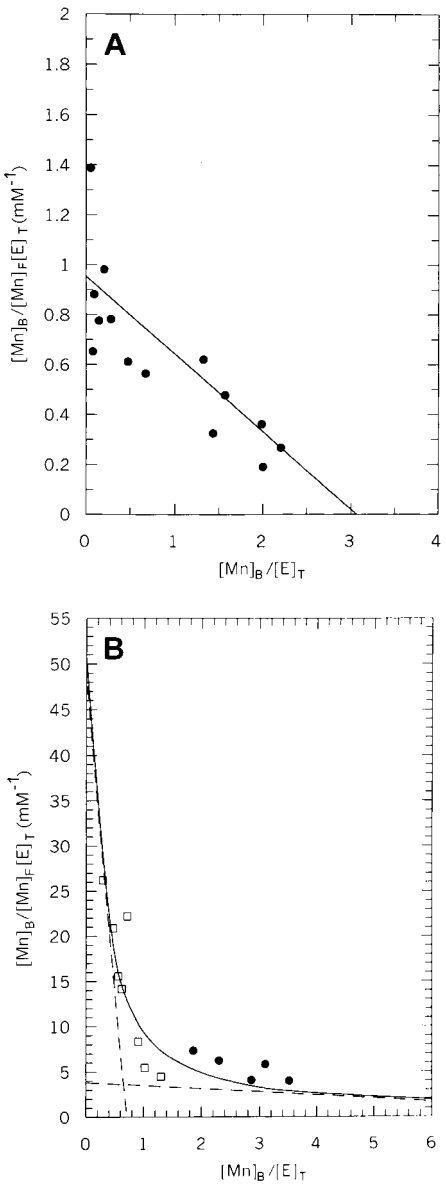

FIGURE 5: Affinities and stoichiometries of Mn^{2+} binding to GDPMH and to the GDPMH−GDP complex. (A) Scatchard plot of Mn^{2+} binding to GDPMH. Enzyme subunit concentrations were 202, 319, or 619 μM, and the concentration of $MnCl_2$ was varied between 72 μM and 10.9 mM. (B) Scatchard plot of Mn^{2+} binding to GDPMH in the presence of GDP. Enzyme subunit and GDP concentrations were both 51 or 101 μM, and the concentration of $MnCl_2$ was varied between 22 and 893 μM. Also present was 80 mM NaHEPES, pH 7.5, $T = 22°$ C. Points in (B) denoted by the (□) symbol are averages of several determinations. The dissociation constants and stoichiometries used to fit these data are given in Table 2.

substrate complex, thus differing from the binding of the Mn^{2+}−NTP substrate to the Mn^{2+} complex of the MutT enzyme (*7*).

The dissociation constant of the binary Mn^{2+}−GDP complex ($K_1 = 0.12 \pm 0.04$ mM) (Table 2) was 53-fold tighter than that of the Mn^{2+}−GDP-mannose complex, likely due to the greater negative charge of GDP. A 1:1 binding stoichiometry of the Mn^{2+}−GDP-mannose complex is indicated by its enhancement factor (ϵ_A), which scales with the molecular weight for small Mn^{2+} complexes (*8*, *18*). Thus, the ratio of molecular weights of the $(H_2O)_4Mn^{2+}$−GDP-mannose and $(H_2O)_4Mn^{2+}$−GDP complexes is 1.28, and the ratio of their ϵ_A values is 1.43 ± 0.20 (Table 4).

Table 4: Enhancement Factors[a] and Metal Binding Stoichiometries (n) of Mn^{2+} Complexes

complex	ϵ_A	ϵ_b	ϵ_T	n
Mn^{2+}−GDP	1.6 ± 0.2			1.0
Mn^{2+}−GDP-mannose	2.29 ± 0.04			1.0[b]
Mn^{2+}−enzyme		11.5 ± 1.2		3.1 ± 0.9
enzyme−Mn^{2+}−GDP			4.9 ± 0.4	0.7 ± 0.2
				10 ± 5[c]

[a] ϵ_A is the enhancement factor for binary metal−substrate or metal−product complexes, ϵ_b is the enhancement factor for the binary metal−enzyme complex, and ϵ_T is the enhancement factor for the ternary enzyme−metal−product complex. [b] Stoichiometry assumed on the basis of the relative values of ϵ_A of $(H_2O)_4Mn^{2+}$−GDP-mannose and $(H_2O)_4Mn^{2+}$−GDP as discussed in the text. [c] Weak sites detected in the titration of Figure 5B.

Ternary Enzyme−Mn^{2+}−GDP Product Complex. Using both EPR and PRR data, Scatchard plot analysis of the binding of Mn^{2+} to the enzyme−GDP complex revealed approximately one tight Mn^{2+} binding site per subunit ($n = 0.7 \pm 0.2$) with a $K_A' = 15 \pm 3$ μM. The binding of GDP thus significantly raised the affinity of the enzyme for Mn^{2+} at one site per subunit, by 213-fold (Table 2). In addition, 10 ± 5 weak, Mn^{2+} binding sites with an average $K_A' = 2.6 \pm 0.4$ mM were found (Figure 5B). An accurate determination of the number of weak Mn^{2+} binding sites on the enzyme was not obtainable due to the large errors in points obtained at high Mn^{2+} concentrations.

PRR titration of the binary enzyme−Mn^{2+} complex with GDP, maintaining all other components constant in concentration (Figure 3B), yielded a dissociation constant (K_3) of GDP from the ternary enzyme−Mn^{2+}−GDP complex of 18 ± 9 μM and an enhancement factor of the ternary complex $\epsilon_T = 4.5 \pm 0.5$. The data of Figure 3B are well fit in the most sensitive curvilinear region of the GDP titration curve. The errors in K_3 and in ϵ_T take into account the less satisfactory fitting at the end of the titration curve, where mixtures of binary Mn^{2+}−GDP and ternary enzyme−Mn^{2+}−GDP complexes were present. A repeat GDP titration at a lower enzyme concentration (401 μM subunits) yielded the same K_3 value (19 ± 9 μM). These K_3 values overlap with the K_I of GDP obtained kinetically (46 ± 27 μM) (Table 3), suggesting this to be the product-inhibited ternary complex. The titration of Figure 3B, together with other measurements of ϵ_T, yielded an average enhancement factor of the ternary complex ($\epsilon_T = 4.9 \pm 0.4$) which was constant with site occupancy and significantly lower than that of the binary complex ($\epsilon_b = 11.5 \pm 1.2$) (Table 4), suggesting the displacement of water ligands on enzyme-bound Mn^{2+} by GDP and the formation of an enzyme−Mn^{2+}−GDP bridge complex. GDP binds more tightly to the enzyme−metal complex than does the GDP-mannose substrate ($K_m^{GDPmann} = 0.32 \pm 0.18$ mM), likely due to the additional negative charge on GDP versus GDP-mannose. On the basis of homology (Figure 1), two arginine residues in addition to the divalent cation are expected to be present in the active site of GDPMH which could facilitate the binding of anionic ligands.

Binary Mg^{2+}Complexes of the Enzyme and Substrate. The dissociation constant of Mg^{2+} from the enzyme was measured directly by a $^1H-^{15}N$ HSQC NMR Mg^{2+} titration experiment which yielded a $K_D = 8.6 \pm 1.5$ mM (Figure 6A). The

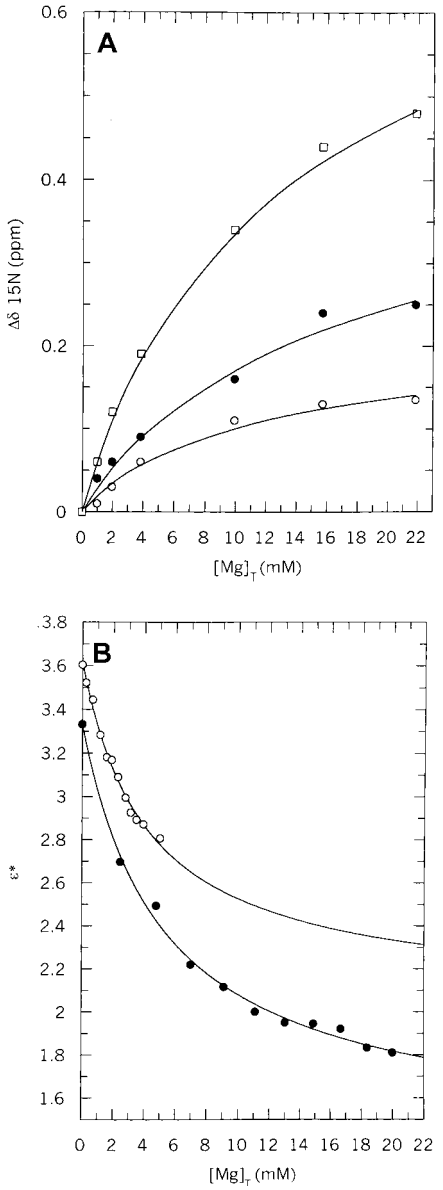

FIGURE 6: Binding of Mg^{2+} to GDPMH. (A) $^1H-^{15}N$ HSQC NMR titration of GDPMH with $MgCl_2$. The initial chemical shifts in ppm for ^1H and ^{15}N were 8.58, 121.42 (○), 8.94, 121.15 (●), and 7.78, 119.48 (□). The curves are fitted to the data using eq 7. (B) PRR titrations of GDPMH with $MgCl_2$ in competition with Mn^{2+}. In the PRR experiment, $MgCl_2$ was titrated into a solution containing enzyme (0.46 mM subunits) and $MnCl_2$ (0.485 mM) in the presence of 80 mM NaHEPES, pH 7.5, keeping the concentrations of enzyme and Mn^{2+} constant (○), yielding a $K_D = 4.6 \pm 0.5$ mM. In the second PRR titration, $MgCl_2$ was directly titrated into a solution containing enzyme and $MnCl_2$ (●), and the 25% dilutions of the enzyme and Mn^{2+} were taken into account in calculating the $K_D = 4.8 \pm 1.1$ mM.

dissociation constant of Mg^{2+} from GDPMH was independently measured by competition with Mn^{2+} bound at the enzyme's three Mn^{2+} sites per subunit (Figure 6B). The decrease in ϵ^* reflecting the decrease in the concentration of enzyme-bound Mn^{2+} with increasing Mg^{2+} concentration was followed in PRR titration experiments and yielded a $K_D = 4.7 \pm 0.8$ mM. The complete displacement of bound Mn^{2+} by Mg^{2+} was confirmed by EPR detection of free Mn^{2+}. The average K_D value of Mg^{2+} (6.0 ± 1.8 mM) overlapped with the kinetically determined K_a value of Mg^{2+} (3.9 ± 1.3 mM) (Tables 1−3).

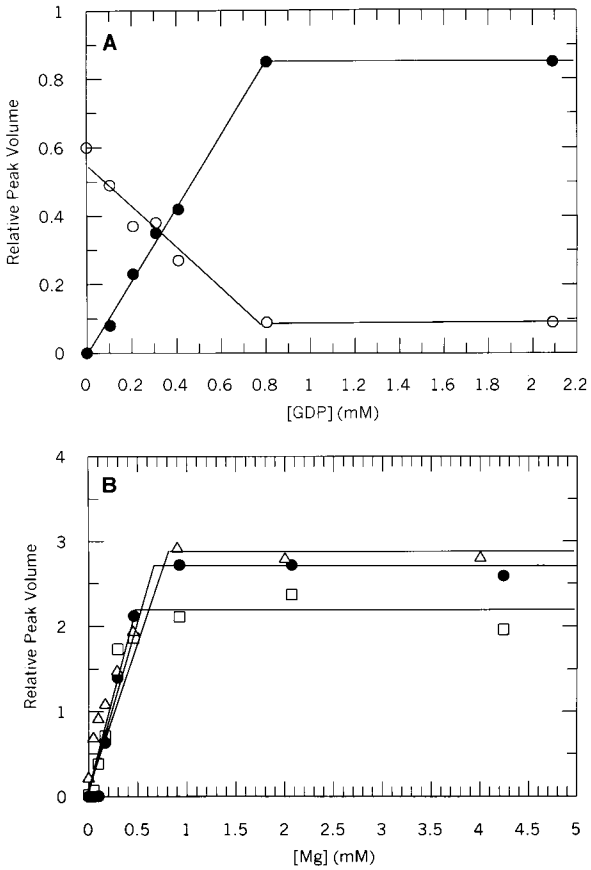

FIGURE 7: $^1H-^{15}N$ HSQC titrations forming the ternary GDPMH−Mg^{2+}−GDP complex. (A) GDP titration of GDPMH (0.98 mM subunits) in the presence of 21.85 mM $MgCl_2$ showing an average binding stoichiometry of 0.8 ± 0.1 GDP binding sites per enzyme monomer in the ternary complex. The ^1H and ^{15}N chemical shifts in ppm are 7.52, 128.61 (○) and 7.73, 127.01 (●). (B) $MgCl_2$ titration of GDPMH (1.02 mM subunits) in the presence of 1.1 mM GDP showing an average binding stoichiometry of 0.7 ± 0.1 Mg^{2+} binding sites per enzyme monomer in the ternary complex. The ^1H and ^{15}N chemical shifts in ppm are 9.74, 129.26 (□), 6.73, 116.39 (●), and 9.58, 131.12 (△). A fourth titration curve at 7.74 and 127.06 ppm overlaps closely with that indicated by (●), also yielding a binding stoichiometry of 0.7 Mg^{2+} binding sites per enzyme monomer.

The dissociation constant (K_1) of the binary Mg^{2+}−GDP-mannose substrate complex was measured by PRR in competition with Mn^{2+}, yielding a $K_1^{Mg^{2+}-GDPmann} = 9.1 \pm 2.0$ mM, which was 1.4-fold greater than the $K_1^{Mn^{2+}-GDPmann}$ (Table 2).

Ternary Enzyme−Mg^{2+}−GDP Complex. The dissociation constant (K_3) of GDP from the ternary enzyme−Mg^{2+}−GDP complex could not be determined in a $^1H-^{15}N$ HSQC NMR titration of the enzyme−Mg^{2+} sample (0.98 mM GDPMH subunits and 21.85 mM Mg^{2+}) with GDP (Figure 7A) because the dissociation constant of GDP was much lower than the enzyme concentration required for such titrations. Accordingly, the HSQC titration revealed slow exchange of the nucleotide, resulting in a change in resonance intensities rather than in chemical shifts. A stoichiometry of 0.8 ± 0.1 tight nucleotide binding sites per enzyme subunit was found, and an upper limit to K_3 of <0.5 mM was estimated.

In a $^1H-^{15}N$ HSQC titration of GDPMH (1.02 mM subunits) and GDP (1.1 mM) with $MgCl_2$, a Mg^{2+} binding stoichiometry of 0.7 ± 0.1 tight binding sites per subunit was detected, based on the appearance of four new reso-

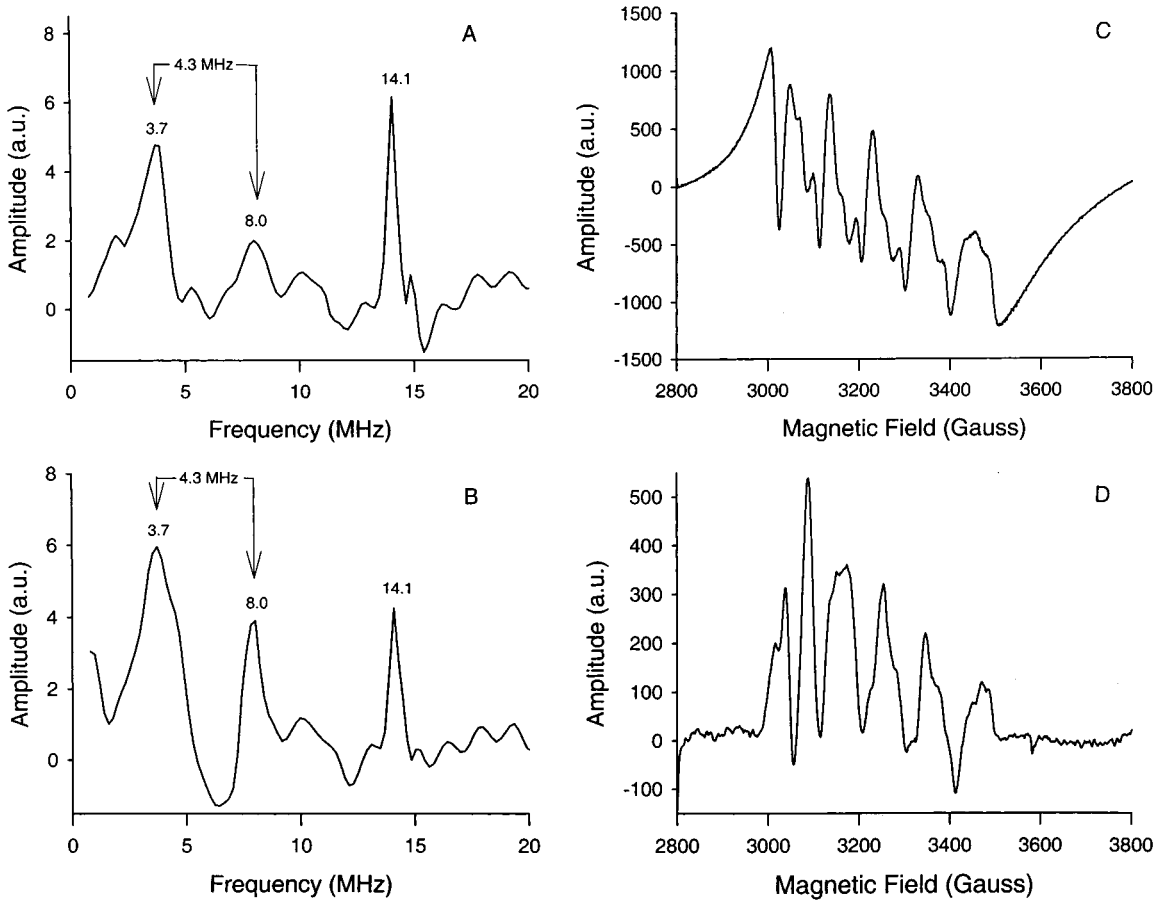

FIGURE 8: Two-pulse ESEEM spectra (A, B) and continuous wave EPR spectra (C, D) of the binary Mn^{2+}−GDP complex (A, C) and of the ternary GDPMH−Mn^{2+}−GDP complex (B, D). The ESEEM data were collected at microwave frequency = 9.25 GHz, magnetic field = 3303 G, τ = 140 ns, τ increment = 5 ns, and temperature = 4 K. The spectra shown in (A) and (B) are Fourier transformations of the normalized time-domain data. The continuous wave EPR spectra in (C) and (D) were collected at microwave frequency = 9.11 GHz, magnetic field = 3300 ± 500 G, microwave power = 10 mW, modulation frequency = 100 kHz, modulation amplitude = 8 G, and temperature = 77 K. The receiver gain of (D) is 4 times that of (C). The samples contained 1.0 mM $MnCl_2$, 2.24 mM GDP, 80 mM NaHEPES, pH 7.5, and 50% (v/v) ethylene glycol. In addition, samples B and D contained 2.9 mM GDPMH subunits.

nances in slow exchange (Figure 7B). The dissociation constant of Mg^{2+} from the ternary enzyme−Mg^{2+}−GDP complex (K_A') was too low to be determined by the HSQC method, but its upper limit was estimated as <0.3 mM. The low binding stoichiometry of Mg^{2+} probably results from the fact that only 9.6% of the enzyme sites were initially occupied by GDP, based on the high dissociation constant (K_S) of GDP (Table 2). Titrations with Mg^{2+} at higher concentrations of GDP were not usable for analysis of the ternary complex because they resulted in the formation of excess binary Mg^{2+}−GDP.

Effects of Ethylene Glycol on the Kinetic Parameters of GDPMH. To determine whether the magnetic diluent, ethylene glycol (50% v/v), used for some of the ESEEM spectra, might alter the enzyme structure, the effects of this solvent on V_{max} and K_m of the enzyme were measured at 22 and 0 °C (Table 5). At 22 °C a 12.6-fold decrease in V_{max} was observed. However, at 0 °C the V_{max} decreased only 5.2-fold, indicating less inhibition at lower temperatures. The effect of ethylene glycol on the K_m of GDP-mannose was similar at both temperatures, showing a 2.5-fold increase at 22 °C and a 3-fold increase at 0 °C.

ESEEM Studies of Mn^{2+} Complexes of GDPMH in H_2O. Panels A and B of Figure 8 show the two-pulse ESEEM spectra of the binary Mn^{2+}−GDP complex and of the ternary enzyme−Mn^{2+}−GDP complex, respectively. Both spectra contain a pair of lines at 3.7 and 8.0 MHz that center around the ^{31}P Larmor frequency (5.7 MHz at 3328 G), indicating a Fermi hyperfine contact interaction of 4.3 ± 0.2 MHz between Mn^{2+} and ^{31}P. Data were also collected at two other magnetic fields for both complexes and showed both of these peaks to shift with the ^{31}P Larmor frequency. For example, for the ternary enzyme−Mn^{2+}−GDP complex, these peaks were resolved at 3.3 and 7.6 MHz at 3128 G (^{31}P Larmor = 5.4 MHz), and at 4.1 and 8.2 MHz at 3528 G (^{31}P Larmor = 6.1 MHz). Therefore, these peaks originate from the coupling of ^{31}P ($I = {}^1/_2$) and the $M_S = \pm{}^1/_2$ transition of Mn^{2+} ($S = {}^5/_2$) (*30*), and the peak-to-peak frequency difference of 4.3 MHz approximates the Fermi contact interaction within the experimental error of ±0.2 MHz. The spectrum of the binary GDPMH−Mn^{2+} complex did not contain either of these signals (not shown). All of the ESEEM

Table 5: Effects of Ethylene Glycol on the Kinetic Parameters of GDPMH at 0 and 22 °C

ethylene glycol (50% v/v)	temp (°C)	V_{max} (unit/mg)	$K_m^{GDPmann}$ (mM)	k_{cat} (s^{-1})
−	0.0	0.031 ± 0.008	0.3 ± 0.1	0.010 ± 0.002
+	0.0	0.006 ± 0.002	0.9 ± 0.4	0.0018 ± 0.0006
−	21.5	0.63 ± 0.08	0.57 ± 0.09	0.19 ± 0.02
+	21.5	0.05 ± 0.03	1.4 ± 0.9	0.015 ± 0.009

experiments with enzyme were done in both the absence and presence of 50% (v/v) ethylene glycol, which did not alter the Fermi contact splitting but in some cases improved the resolution.

The Fermi contact splitting provides direct evidence for inner sphere coordination of GDP to Mn^{2+} in both the binary Mn^{2+}−GDP and the ternary enzyme−Mn^{2+}−GDP complexes. Although the magnitude of the hyperfine coupling is the same within experimental error for both complexes, the increase in intensity of the ^{31}P signal and the decrease in intensity of the ^{1}H signal at 14.1 MHz in the ternary complex (Figure 8B) indicate that the Mn^{2+} sites are not identical and support the formation of an enzyme−Mn^{2+}−GDP bridge complex. The decrease in intensity of the ^{1}H signal indicates that water ligands in the binary Mn^{2+}−GDP complex were replaced by ligands from the protein in the ternary complex and/or decreased solvent accessibility of the Mn^{2+} site in the ternary complex.

Independent evidence for ternary complex formation is provided by continuous wave EPR spectra (Figure 8C,D). Altered relative intensities of the six ^{55}Mn ($I = {}^5/_2$) hyperfine lines and decreased splittings resolved for each in the spectrum of the ternary enzyme−Mn^{2+}−GDP complex (Figure 8D) as compared to that of the binary Mn^{2+}−GDP complex (Figure 8C) indicate a change in the ligand symmetry at the Mn^{2+} site (*31*).

The equal Fermi contact splitting within experimental error in the binary Mn^{2+}−GDP and ternary enzyme−Mn^{2+}−GDP complexes (4.3 ± 0.2 MHz) suggests similar interactions of GDP with Mn^{2+} in both complexes.

^{2}H ESEEM Studies of Mn^{2+} Complexes of GDPMH. A previously established ^{2}H ESEEM method (*9*) was used to compare the average number of water ligands on Mn^{2+} in the three binary enzyme−Mn^{2+} complexes with that in the ternary enzyme−Mn^{2+}−GDP complex. From their X-ray structures, Mn^{2+}-EDTA shows one water ligand on the metal, and Mn^{2+}-DTPA shows no water ligands (*26*). Assuming that the modulations due to ambient D_2O in both complexes are the same (*9*), the ratio of the ^{2}H ESEEM of Mn^{2+}-EDTA with that of Mn^{2+}-DTPA gives the ^{2}H ESEEM of the single Mn^{2+}-bound D_2O in Mn^{2+}-EDTA, which can then be used as a standard to estimate the number of D_2O ligands in other Mn^{2+} complexes.

Panels A and B of Figure 9 respectively show the Fourier transformations of the ratio of the ^{2}H ESEEM of Mn^{2+}-EDTA to that of Mn^{2+}-DTPA and of the second power of this ratio. The intensity of the peak at the ^{2}H Larmor frequency (2.2 MHz) represents respectively one (Figure 9A) and two (Figure 9B) Mn^{2+}-bound D_2O ligands. [Note that the ESEEM function is a product of all coupled nuclei (*9* and references cited therein).] When the ^{2}H ESEEM of the ternary enzyme−Mn^{2+}−GDP complex was ratioed with those of the binary enzyme−Mn^{2+} complexes, the Fourier transformation (Figure 9C) shows a negative peak at the ^{2}H Larmor frequency with an intensity very similar to that of the positive peak in Figure 9B. These results demonstrate that Mn^{2+} bound in the ternary 1:1:1 enzyme−Mn^{2+}−GDP complex coordinates two fewer D_2O ligands than does the average Mn^{2+} in the three binary enzyme−Mn^{2+} complexes, assuming that the contributions of ambient D_2O to the ^{2}H ESEEM of both systems are the same. This assumption was

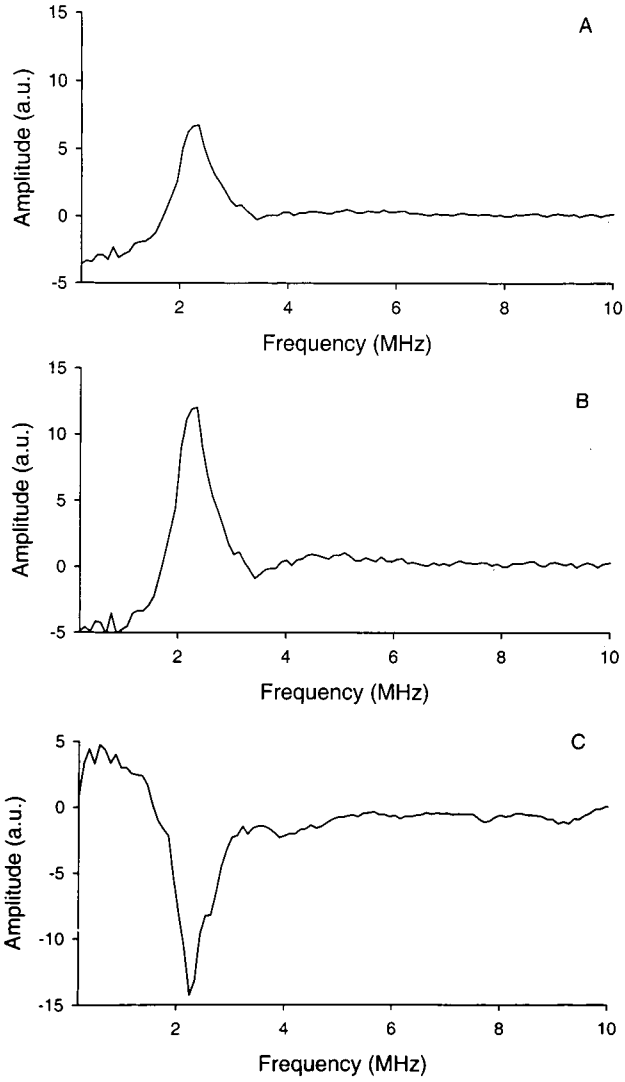

FIGURE 9: Analysis of ^{2}H ESEEM spectra of model Mn^{2+} complexes and of the binary GDPMH−Mn^{2+} and ternary GDPMH−Mn^{2+}−GDP complexes. (A) Fourier transformation of the ratio of the ^{2}H ESEEM of Mn^{2+}-EDTA with that of Mn^{2+}-DTPA. (B) Fourier transformation of the square of the ratio of the ^{2}H ESEEM of Mn^{2+}-EDTA with that of Mn^{2+}-DTPA. (C) Fourier transformation of the ratio of the ^{2}H ESEEM of the ternary GDPMH−Mn^{2+}−GDP complex with that of the binary GDPMH−Mn^{2+} complex. All time-domain data were collected using the three-pulse sequence, with microwave frequency = 9.4 GHz, magnetic field = 3325 G, $\tau = 140$ ns, initial $T = 60$ ns, T increment = 10 ns, and temperature = 4 K. For (A) and (B), the samples contained 1.2 mM EDTA or DTPA, 1.0 mM $MnCl_2$, and 80 mM NaHEPES, pH 7.5, in D_2O (99.9%), and 50% (v/v) d_2-ethylene glycol. For (C), the samples contained 2.9 mM GDPMH subunits with or without 2.24 mM GDP, 1.0 mM $MnCl_2$, and 80 mM NaHEPES, pH 7.5, in D_2O (99.9%), and 50% (v/v) d_2-ethylene glycol.

previously found to be valid in comparing binary and ternary Mn^{2+} complexes of staphylococcal nuclease (*9*). The binary Mn^{2+}−ADP complex in solution shows bidentate chelation of the metal ion by both the α- and β-phosphoryl groups of the nucleotide (*32*). A similar coordination is also likely for Mn^{2+}−GDP. The present finding that the ternary enzyme−Mn^{2+}−GDP complex contains two fewer D_2O ligands than the average Mn^{2+} in the three binary enzyme−Mn^{2+} complexes is consistent with bidentate chelation of the enzyme-bound Mn^{2+} by GDP. The same results were found using samples not containing ethylene glycol.

DISCUSSION

The kinetic, metal binding, and magnetic resonance data in this paper indicate that GDPMH requires one divalent cation per active site for catalytic activity, which bridges the enzyme to the leaving group, GDP. The most compelling observations supporting a single, bridging metal at the active site of GDPMH are that the enzyme−GDP product complex binds only one Mn^{2+} per subunit tightly ($K_A' = 15 \pm 3\ \mu M$) (Figure 5B) and that this enzyme-bound Mn^{2+} interacts directly with the phosphates of bound GDP as detected by Fermi contact splitting of the phosphorus resonance in the ESEEM spectrum (Figure 8B). In addition, a large number of weak Mn^{2+} binding sites are detected on the enzyme, but these are remote (≥10 Å) from the tight binding site, on the basis of the constant value of ϵ_T as a function of metal occupancy (*8*). Further, while the free enzyme binds three Mn^{2+} ions per subunit with average dissociation constants ($K_D = 3.2 \pm 1.0$ mM) that agree with the kinetically determined activator constant ($K_a = 3.9 \pm 1.1$ mM), these metal ions are also remote from each other, on the basis of the constant value of ϵ_b as a function of occupancy (*8*). The binary enzyme−Mn^{2+} complexes bind only one GDP per subunit to form a tight 1:1:1 ternary enzyme−Mn^{2+}−GDP complex. The dissociation constant of GDP from this ternary complex ($K_3 = 18 \pm 9\ \mu M$) overlaps with the K_I of GDP ($K_I = 46 \pm 27\ \mu M$) (Figure 3B, Table 3), indicating this complex to correspond to the product complex in the enzymatic reaction. Similar kinetic behavior and stoichiometric binding of GDP and Mg^{2+} were found with the Mg^{2+}-activated enzyme (Figure 7, Tables 1 and 2).

No threshold concentration of divalent cation was found kinetically in the activation of GDPMH, unlike that observed with the MutT enzyme, which requires two divalent cations with unequal affinities, a tightly bound metal on the substrate, and a more weakly bound metal on the enzyme. Accordingly, the MutT enzyme shows a threshold concentration in metal activation (*7*). The GDPMH−substrate complex shows a kinetically determined affinity for Mn^{2+} ($K_m^{Mn^{2+}} = 0.32 \pm 0.18$ mM) (Table 1) which is 19-fold tighter than the dissociation constant of the binary Mn^{2+}−substrate complex ($K_1 = 6.2 \pm 0.4$ mM) (Table 2). Similarly, the $K_m^{Mg^{2+}}$ is 13-fold tighter than the dissociation constant (K_1) of the binary Mg^{2+}−GDP-mannose complex (Tables 1 and 2). Hence, the weak binding of an additional divalent cation to the substrate is not necessary for catalysis. By the same argument, Mn^{2+} binding to one or more of the additional weak sites on GDPMH is not required for catalysis.

The formation of a metal bridge enzyme−Mn^{2+}−product complex is further supported by the mutual tightening of binding by 2 orders of magnitude of Mn^{2+} and GDP as detected by GDP and metal binding studies (Table 2). The observation that the enhancement factor of the ternary enzyme−Mn^{2+}−GDP complex ($\epsilon_T = 4.9 \pm 0.4$) is significantly lower than the average enhancement factor of the binary enzyme−Mn^{2+} complexes ($\epsilon_b = 11.5 \pm 1.2$) indicates that the binding of GDP has decreased the access of water ligands to the paramagnetic metal ion (Table 4), further supporting a metal bridge complex. Similarly, the formation of a metal bridge enzyme−M^{2+}−substrate complex is supported by the order of magnitude mutual tightening of binding of the divalent cation and the substrate GDP-mannose detected kinetically for both the Mn^{2+}- and Mg^{2+}-activated enzymes (Table 1).

However, these observations are indirect and subject to alternative explanations, such as the formation of second-sphere enzyme−$Mn^{2+}(H_2O)_n$GDP-mannose and enzyme−$Mn^{2+}(H_2O)_n$GDP complexes, which could also show mutual tightening of metal and nucleotide binding and decreased accessibility of solvent to the metal in the respective ternary complexes. Indeed, the similar K_m values of Mn^{2+} and Mg^{2+} and the similar K_m values of GDP-mannose and K_I values of GDP found with both the Mn^{2+}- and Mg^{2+}-activated enzymes (Table 1) raise the possibility of second-sphere complexes in which there is no direct contact between the enzyme-bound divalent cation and the nucleotide. To resolve this ambiguity, it was necessary to search more directly for the formation of a metal bridge complex. This was accomplished by the ESEEM measurements which detected unequivocally the direct coordination of one or more phosphoryl groups of GDP by the enzyme-bound Mn^{2+}. Such coordination was revealed by the Fermi contact splitting (4.3 ± 0.2 MHz) of the phosphorus signal in the Fourier transformed spectrum of the enzyme-bound Mn^{2+}, indicating delocalization of the unpaired electrons of Mn^{2+} to phosphorus nuclei (Figure 8B). Such delocalization can occur only through chemical bonds (*9*, *33*). The magnitude of the Fermi contact splitting is very similar to values found for other binary Mn^{2+}−nucleotide and ternary enzyme−Mn^{2+}−nucleotide complexes (*9*, *30*).

Direct coordination of GDP was also supported by ^2H ESEEM (Figure 9), which showed the loss of two D_2O ligands of Mn^{2+}, on average, on converting the mixture of three binary enzyme−Mn^{2+} complexes to the single ternary enzyme−Mn^{2+}−GDP complex, consistent with bidentate coordination of the enzyme-bound Mn^{2+} by GDP, as in the binary Mn^{2+}−ADP complex (*32*). A remaining water ligand on Mn^{2+} in the ternary complex is indicated by its enhancement factor (ϵ_T) of 4.9 ± 0.4 (Table 4). Since Mn^{2+} generally prefers octahedral coordination (*34*), the enzyme likely donates three ligands to Mn^{2+} to complete its coordination sphere.

Mechanistically, the fact that the enzyme-bound divalent cation coordinates the GDP product suggests that it also coordinates the GDP moiety of the GDP-mannose substrate, thereby promoting the departure of the GDP leaving group. A metal bridge enzyme−M^{2+}−substrate complex is indicated by the order of magnitude mutual tightening of binding of the divalent cation and substrate detected kinetically (Table 1). Such a complex is shown in the proposed mechanism of Figure 10A. This mechanism is compared with those previously proposed for MutT (Figure 10B) (*5*, *35*) and for Ap_4A pyrophosphatase (Figure 10C) (*8*).

GDPMH differs from other Nudix enzymes in four ways. First and foremost, it catalyzes nucleophilic substitution at carbon rather than at phosphorus (*1*). Second, it has a slightly altered Nudix sequence motif at the active site (Figure 1) (*12*). Third, GDPMH requires only *one* divalent cation for activity unlike the prototype Nudix enzyme MutT from *E. coli*, which requires two (Figure 10B) (*7*), or Ap_4A pyrophosphatase from *Bartonella bacilliformis*, which requires three (Figure 10C) (*8*). This difference in metal requirement may be attributable to the lower charge of the GDP-mannose substrate (−2) in comparison to the NTP substrate of MutT

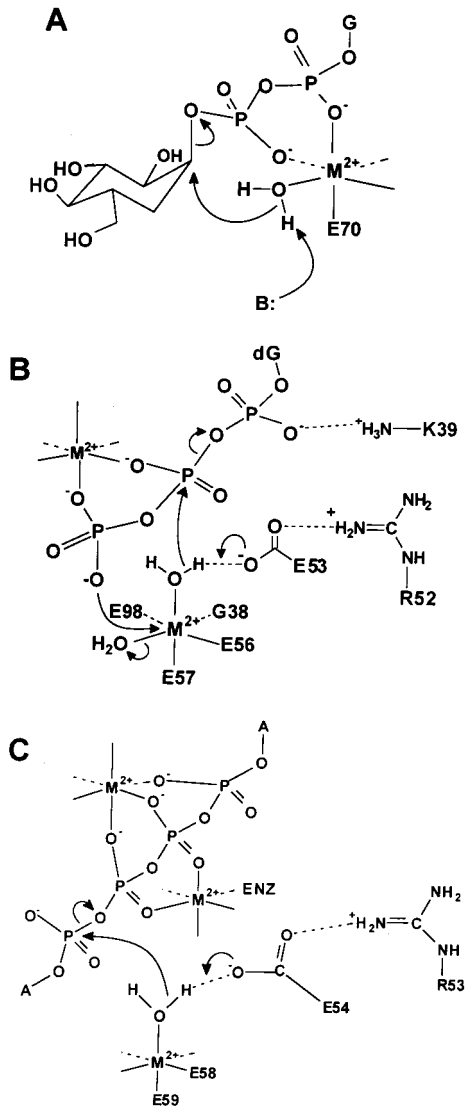

FIGURE 10: Proposed roles of divalent cations in the mechanisms of Nudix enzymes. (A) Role of one metal ion in the active site of GDPMH. (B) Roles of two metal ions in the active site of MutT (*7*, *35*). (C) Roles of three metal ions in the active site of Ap_4A pyrophosphatase (*8*). The residue numbering scheme is that of the *L. angustifolius* L. Ap_4A pyrophosphatase (*38*).

(−4) and the Ap_4A substrate of Ap_4A pyrophosphatase (−4) and to differences in the numbers of charged residues in the respective active sites. Fourth, unlike other Nudix enzymes (*7*, *8*) and numerous kinases, the kinetic and binding parameters of GDPMH are insensitive to a change in the divalent cation activator from Mn^{2+} to Mg^{2+} (Tables 1 and 2). This behavior is unusual because of the order of magnitude greater affinity of Mn^{2+} for ligands in general (*27*), suggesting that other interactions at the active site of GDPMH strongly influence dissociation constants and catalytic rates. Indeed, mutational studies, which will be the subject of a future paper, show the importance of arginine residues at the active site of GDPMH (Figure 1) which may also interact with the pyrophosphate moiety of GDP and GDP-mannose.

REFERENCES

1. Legler, P. M., Massiah, M. A., Bessman, M. J., and Mildvan, A. S. (2000) *Biochemistry 39*, 8603−8608.
2. Bessman, M. J., Frick, D. N., and O'Handley, S. F. (1996) *J. Biol. Chem. 271*, 25059−25062.
3. Weber, D. J., Bhatnagar, S. K., Bullions, L. C., Bessman, M. J., and Mildvan, A. S. (1992) *J. Biol. Chem. 267*, 16939−16942.
4. Cartwright, J. L., Britton, P., Minnick, M. F., and McLennan, A. G. (1999) *Biochem. Biophys. Res. Commun. 256*, 474−479.
5. Lin, J., Abeygunawardana, C., Frick, D. N., Bessman, M. J., and Mildvan, A. S. (1997) *Biochemistry 36*, 1199−1211.
6. Swarbrick, J. D., Bashtannyk, T., Maksel, P., Zhang, S. R., Blackburn, G. M., Gayler, K. R., and Gooley, P. R. (2000) *J. Mol. Biol. 302*, 1165−1177.
7. Frick, D. N., Weber, D. J., Gillespie, J. R., Bessman, M. J., and Mildvan, A. S. (1994) *J. Biol. Chem. 269*, 1794−1803.
8. Conyers, G. B., Wu, G., Bessman, M. J., and Mildvan, A. S. (2000) *Biochemistry 39*, 2347−2354.
9. Serpersu, E. H., McCracken, J., Peisach, J., and Mildvan, A. S. (1988) *Biochemistry 27*, 8034.
10. Coffino, A. R., and Peisach J. (1996) *J. Magn. Reson., Ser. B 111*, 127−134.
11. Weber, D. J., Gittis, A. G., Mullen, G. P., Abeygunawardana, C., Lattman, E. E., and Mildvan, A. S. (1992) *Proteins 13*, 275−287.
12. Frick, D. N., Townsend, B. D., and Bessman, M. J. (1995) *J. Biol. Chem. 270*, 24086−24091.
13. Gill, S. C., and von Hippel, P. H. (1989) *Anal. Biochem. 182*, 319−326.
14. Mildvan, A. S., and Engle, J. L. (1972) *Methods Enzymol. 26C*, 654−683.
15. Cohn, M., and Townsend, J. (1954) *Nature 173*, 1090−1091.
16. Reed, G. H., and Markham, G. D. (1984) in *Biological Magnetic Resonance* (Berliner, L., and Reuben, J., Eds.) Vol. 6, pp 73−142, Plenum Press, New York.
17. Eisinger, J., Shulman, R. G., and Szymanski, B. M. (1962) *J. Chem. Phys. 36*, 1721.
18. Mildvan, A. S., and Cohn, M. (1970) *Adv. Enzymol. 33*, 1−70.
19. Mildvan, A. S., and Gupta, A. S. (1978) *Methods Enzymol. 59G*, 322−369.
20. Marion, D., Driscol, P. C., Kay, L. E., Wingfield, P. T., Bax, A., Gronenborn, A. M., and Clore, G. M. (1989) *Biochemistry 28*, 6150−6156.
21. McCracken, J., Peisach, J., and Dooley, D. M. (1987) *J. Am. Chem. Soc. 109*, 4064−4072.
22. Bender, C. J., Rosenzweig, A. C., Lippard, S. J., and Peisach, J. (1994) *J. Biol. Chem. 269*, 15993−15998.
23. Britt, R. D., and Klein, M. P. (1987) *J. Magn. Reson. 74*, 535−540.
24. Mims, W. B., and Peisach, J. (1976) *Biochemistry 15*, 3863−3869.
25. Peisach, J., Mims, W. B., and Davis, J. (1979) *J. Biol. Chem. 254*, 12379−12384.
26. Stezowski, J. J., and Hoard, J. L. (1984) *Isr. J. Chem. 24*, 323−334.
27. Dawson, R. M. C., Elliot, D. C., Elliot, W. H., and Jones, K. M. (1986) *Data for Biochemical Research*, Oxford University Press, New York.
28. Dixon, M. (1972) *Biochem. J. 129*, 197−202.
29. Lin, J., Abeygunawardana, C., Frick, D. N., Bessman, M. J., and Mildvan, A. S. (1996) *Biochemistry 35*, 6715−6726.
30. Larsen, R. G., Halkides, C. J., and Singel, D. J. (1993) *J. Chem. Phys. 98*, 6704−6721.
31. Coffino, A. R., and Peisach, J. (1996) *J. Magn. Reson. 111*, 127−134.
32. Cohn, M., and Hughes, T. R. (1962) *J. Biol. Chem. 237*, 176−181.
33. LoBrutto, R., Smithers, G. W., Reed, G. H., Orme-Johnson, W. H., Pan, S. L., and Leigh, J. S. (1986) *Biochemistry 25*, 5654−5660.
34. Bock, C. W., Katz, A. K., Markham, G. D., and Glusker, J. P. (1999) *J. Am. Chem. Soc. 121*, 7360−7372.

35. Harris, T. K., Wu, G., Massiah, M. A., and Mildvan, A. S. (2000) *Biochemistry 39*, 1655−1674.
36. Rost, B., and Sander, C. (1993) *J. Mol. Biol. 232*, 584−599.
37. Weber, D. J., Abeygunawardana, C., Bessman, M. J., and Mildvan, A. S. (1993) *Biochemistry 32*, 13081−13088.
38. Maksel, D., Gooley, P. R., Swarbrick, J. D., Guranowski, A., Gange, C., Blackburn, G. M., and Gayler, K. R. (2001) *Biochem. J. 357*, 399−405.

BI012118D